View metadata, citation and similar papers at core.ac.uk
brought to you by CORE
provided by Digital.CSIC

Structure of Thermoreversible Poly(vinyl alcohol) Cryo-Hydrogels as studied by Proton Low Field NMR Spectroscopy

J. L. Valentin*[a,b], D. López[b], R. Hernández[b], C. Mijangos[b], K. Saalwächter[a]

[a] *Martin-Luther-Universität Halle-Wittenberg, Institut für Physik; Friedemann-Bach-Platz 6, D-06108 Halle (Germany)*
[b] *Institute of Polymer Science and Technology (CSIC), C/ Juan de la Cierva 3, 28006-Madrid (Spain)*
**e-mail:jlvalentin@ictp.csic.es*

ABSTRACT

The network structure of Poly(vinyl alcohol) (PVA) hydrogels obtained by freezing-thawing cycles was investigated by solid state ^{1}H low field NMR spectroscopy. By application of multiple-quantum NMR experiments, we obtain information about the segmental order parameter, which is directly related to the restrictions to chain motion (crosslinks) formed upon gelation. These measurements indicate that the network mesh size, as well as the relative amount of non-elastic defects (i.e. non-crosslinked chains, dangling chains, loops) decreases with the number of freezing-thawing cycles, but it is independent of the polymer concentration. The formation of the PVA network is accompanied by an increasing fraction of polymer with fast magnetization decay (~20μs). The quantitative study of this rigid phase with a specific refocusing pulse sequence shows that it is composed of a primary crystalline polymer phase (around 5%), which constitutes the main support of the network structure and determines the mesh size, and a secondary population of more imperfect crystallites, which increase the number of elastic chain segments in the polymer gel but does not affect the average network mesh size appreciably. Correspondingly, progressive melting of the secondary crystallites with increasing temperature does not affect the network mesh size but only the amount of network defects, and melting of the main PVA crystallites at around 80 ºC leads to destruction of the network gel and formation of an isotropic PVA solution.

Key words: Physical gels, time-domain NMR, multiple-quantum NMR, magic-sandwich echo.

INTRODUCTION

Poly(vinyl alcohol) (PVA) is a biocompatible polymer with a great variety of biomedical and pharmaceutical applications[1-4]. PVA in aqueous solution is able to form chemical or physical gels under a variety of conditions[4-7].

The physical gelation capacity of PVA solutions has been well know for a long time[8-10], however the preparation of hydrogels by repeated freezing-thawing cycles has attracted renewed interest [3-4,11-17]. The high degree of swelling in water, rubbery elasticity, chemical and mechanical stability, a porous fibrilar network structure, and lack of toxicity makes freeze/thaw PVA hydrogels an attractive polymer matrix for biotechnological applications[11-17].

To understand the origin of these properties, and therefore the bio-applicability of this material[11-17], it is necessary to study the physical gelation process produced by the freezing/thawing cycles, as well as the formed network structure[18-20]. Komatsu el al.[10] investigated the phase diagram of the water/PVA binary system. According to this diagram, gelation occurs with or without spinodal decomposition according to the polymer concentration and temperature. The process seems to start with a clustering of chains[21-22] caused primarily by association of polar groups of the dissolved polymer, followed by polymer crystallization. This means that the physical crosslinks, which are responsible for the network formation, could be formed by different processes, such as hydrogen bonding, polymer crystallization, and in some cases (depending on the gelation conditions), phase separation[11].

In addition, the application of freezing-thawing cycles to PVA solutions leads to the formation of heterogeneous networks with different morphology and properties as compared to non-frozen gel systems. Peppas et al. were the pioneers in the development of this type of polymer cryogels[7]. In earlier work, they attribute the gel formation to a partial crystallization

of chain segments into microcrystalline structures. X-ray diffraction studies[23-24] confirm that polymer crystallites act as junctions points. However the intensity of the diffraction maximum corresponding to the 101 reflection is only clear for PVA hydrogels with high polymer content[10,24]. For hydrogels with 10 to 15% polymer, solid state NMR was used to identify and quantify the crystalline phase[15,25], although X-ray analysis is also possible[26].

Most recent works show that gelation by freeze/thaw processing forms heterogeneous networks of interconnected micro- and macro-pores. Willcox et al.[25], in an exhaustive study using transmission electron microscopy images and NMR, showed the formation of networks either with rounded pore morphology and/or fibrillar network morphology, depending on the number of cycles as well as ageing. They attribute the formation of crosslinks to a kinetically frustrated crystallization in the first freezing cycle. After this process, subsequent cycles (or ageing processes) lead to the creation of new (secondary) crystallites and the growing of the primary crystals, however the mesh spacing changes slightly. This fact seems to indicate that the average distance between the primary crystallites formed during the first thermal treatment constitutes the main controlling factor for the network structure.

In addition, Auriemma and coworkers in a series of works[14-15,26-27] showed that the porous structure originates from freezing in the first step because of the incomplete crystallization of water. The polymer concentration in this unfrozen water phase is higher than in the original solution and the polymer network is formed within this microphase because of PVA crystallization. The crosslink points are therefore constituted of polymer crystallites, and the formed gels could be described by a bicontinuous structure of polymer-rich and polymer-poor regions. In contrast, Hernández et al., based on DSC measurements, also inferred the possibility of the existence of covalent crosslinks between the polymer chains, brought about by the formation of radicals due to strong local shear during water crystal growth[30-32].

Summing up, the PVA hydrogels obtained by freezing-thawing cycles appear to be constituted by a very complicated network structure based on different phenomena, i.e.

crystallization, hydrogen bonding, liquid-liquid phase separation and covalent bounds. Therefore, a complete analysis of this structure requires the use of different characterization techniques. However most of them require the manipulation of the hydrogel sample, provoking changes in the original structure. For example, the use of chromatographic techniques or scattering techniques to measure molecular weight or cluster size requires the dilution of the gel[21] (although it was shown that it is possible). Mechanical measurements have the limitation of water evaporation at higher temperatures[31]. The cryo-TEM technique has the inconvenience of handling difficulties in order to avoid artifacts[25]. To study the crystallite content, very useful techniques such as differential scanning calorimetry (DSC) as well as X-ray diffraction are challenged by a sensitivity problem in dilute samples; for this reason, sometimes measurements were made in dry samples[33]. In this vein, solid state NMR is a powerful tool to study polymer networks[34-35] but it has not been extensively used in this field.

The focus of this work is the use of a low-field NMR spectrometer to analyze in detail the structure of the PVA gel as a function of the freezing/thawing cycles, checking all the structural models suggested in the literature. In addition, melting process that transforms these physical gels into isotropic solutions of PVA in water was also studied. Importantly, we focus on detecting protons, such that sensitivity, even at the low concentrations under study, is not a serious issue. The use of an un-expensive low field NMR spectrometer on as-prepared samples to study this complex matrix has the advantage that several of the cited inconveniences in sample characterization are avoided. By using different NMR methodologies, we are able to carry out a complete and quantitative study of the complex structure exhibited by the PVA gels: Multiple quantum (MQ) NMR allows us to gain direct access to residual dipolar coupling constants that persist because of the existence of crosslinks and other topological constrains[37-39]. Therefore, this experimental procedure is a powerful tool to quantify the gelation process[40], and gives us quantitative detail not only on the

microstructure,[41] but also the dynamics[42] of the forming and final gel, that is, a complete picture of the network structure evolution, depending on, for example, the number of freezing/thawing cycles. In addition, we used pulsed mixed magic-sandwich echo experiments that provide a near-quantitative refocusing of the rigid contribution to the initial part of the free induction decay (FID),[43] and allow for an essentially quantitative determination of the crystallinity.

EXPERIMENTAL PART

Materials and sample preparation

Poly(vinyl alcohol) was obtained from Aldrich. The sample is >99% hydrolyzed, has a weight average molecular weight of 94000 g/mol, and a tacticity syndio = 17.2%, hetero = 54.1% and iso = 28.7%. PVA was dissolved in deuterated water (with polymer concentration of 10 and 20% g/ml) at 80°C under continuous stirring to avoid inhomogeneities and local gelation. Solutions were stored at 80°C overnight and then they were cooled to room temperature for 1 hour. Then PVA solutions were introduced in 10 mm OD NMR tubes and flame-sealed in order to avoid variation in the water content. Two technical considerations are important at this point: i) the quantity of sample inside the tube has to be smaller than ~8 mm height and located in the center of the rf coil in order to ensure good rf field (B_1) homogeneity. ii) The length of the NMR tube should be as short as possible for good control of the temperature. This is important because in this way the whole tube can be inserted into the probe head, thus avoiding possible temperature gradients due to heat conduction.

Physical PVA hydrogels were obtained by repetition of freezing-thawing cycles of solutions inside the sealed tubes, consisting in 1 hour cooling to -32°C and 1 hour thawing at room temperature. After this process, samples were immediately inserted in the NMR spectrometer and measured to avoid the effect of ageing. In some cases (specified below), the

first freezing cycle was extended to around 12 hours (overnight), and subsequent cycles were 3 hours long.

Solid-state ^{1}H nuclear magnetic resonance

Solid-state ^{1}H NMR spectroscopy is a powerful and widely used experimental technique in the field of polymer science[34]. In recent years, the use of un-expensive and easy to use low field spectrometers[37,44-45] has taken the attraction of scientists because they certainly produce quantitative results on polymer structure and dynamics, albeit of course without chemical resolution. Based on different experiments, applications include quantitative studies on polymer network structure[37] and polymer crystallization[43], i.e. the main topics of this study. In this work, experiments were carried out on a Bruker minispec mq20 spectrometer operating at 0.5 T with 90º pulses of 1.7 µs length and dead time of 12 µs.

^{1}H multiple quantum (MQ) NMR. MQ spectroscopy is one of the most versatile and robust quantitative techniques to investigate not only the structure but also the dynamics of polymer networks[37]. In solution, the fast segmental motion of the polymer chains through the different accessible conformations is isotropic and completely averages the dipolar coupling interaction typical for solid-state spectra. However constraints, irrespective of their nature (e.g. crosslinks, entanglements or chain packing), lead to non-isotropic segmental fluctuations and therefore to the persistence of a weak residual dipolar coupling (D_{res}),[46-48] which is our central NMR observable. In other words, the measured effect relies on the orientation dependence of the fluctuating dipolar coupling tensor with respect to the magnetic field, which can be described by an orientation autocorrelation function of the individual chain segments. Fast segmental dynamics (in the range of ns-µs) lead to a loss of correlation down to a plateau value that is related to the existence of preferential local orientation generated by the existence of crosslinks. In fact, the measurable D_{res} is directly proportional to

a local dynamic order parameter of the polymer backbone[37], which is defined as a time average of the over the fluctuations of the segment-fixed dipolar tensor over the time until the plateau region is reached. It connects the experimental observable with the network parameters:

$$S_b = k\frac{D_{res}}{D_{stat}} = \frac{3}{5}\frac{r^2}{N} \quad (1)$$

Here, D_{stat} is the segmental averaged dipolar coupling constant in the static limit and k a rescaling factor that take into account the fast dynamics (in the range of ps) inside the statistical (Kuhn) segments. The NMR observable is related to r, i.e. the ratio of the end-to-end vector to its average unperturbed melt state ($r^2=\boldsymbol{r}^2/\langle\boldsymbol{r}^2\rangle_0$), and to N, the number of statistical segments between constrains.

A variety of NMR experiments[36,49-52] was used to detect residual dipolar couplings in order to monitor gelation processes, and recently, proton MQ NMR has evolved as the most powerful tool to obtain a direct measurement of D_{res}, and even its distribution.[37-39,53] Details on the pulse sequence as well as the data analysis are already published elsewhere[37,40,54]. Here we point out some relevant details for the current investigation.

Temperature usually plays an important role in MQ measurements,[42] because as mentioned previously, the order parameter should be obtained as an average of the segmental fluctuations over all the possible conformations on the experimental timescale (less than ms). Therefore, the temperature is required to be far above the polymer glass transition temperature T_g in order to ensure that the segmental dynamics is fast enough in order to sweep out the whole conformational space between topological constraints and achieve full averaging. If this is not the case, the obtained D_{res} (and therefore the number of junctions in the network) will be overestimated[40]. In this work, the studied samples are hydrogels, therefore the dissolved state of the polymer chain ensures that the segmental dynamics is indeed fast enough in order to detect the order parameter in the plateau regime even at room temperature.

In a similar vein as in traditional transverse relaxation experiments, the analyzed result of the MQ experiment is a time-dependent, but normalized double-quantum (DQ) signal function, I_{nDQ}, that has the advantage of being independent of any temperature-dependent true relaxation (decay) effect. It is dominated by the dipolar interactions and independent of the polymer dynamics. For this purpose, the directly measured experimental DQ build-up curve (I_{DQ}) must be relaxation-corrected by use of the also measured reference intensity (I_{ref}). Initially, I_{ref} not only contains signal from the dipolar-coupled network chains, but also from uncoupled, isotropically mobile components such as sol, dangling chains, etc. The total MQ magnetization ($I_{\Sigma MQ}$) needed for normalization is the sum of I_{DQ} and I_{ref}, but only after subtracting the non-network contributions. This fraction has a slower relaxation and can easily be identified (Figure 1(a)). In the studied hydrogels, even though we used deuterated water to dissolve the polymer, we found non-negligible water signal, resulting from actual residual water and exchanged –OH protons. Therefore, we had to identify and subtract two exponential long-time contributions to $I_{\Sigma MQ}$, i.e. the non-coupled fraction of polymer chains (B fraction in eq. 2), and the solvent signal (fraction C), which relax with longer relaxation times ($T_{2C}^{*} >> T_{2B}^{*}$):

$$I_{\Sigma MQ} = I_{DQ} + I_{ref} - Be^{-2\tau_{DQ}/T_{2B}^{*}} - Ce^{-2\tau_{DQ}/T_{2C}^{*}} \tag{2}$$

This corrected quantity is used to normalize the DQ intensity (see Figure 1(b)),

$$I_{nDQ} = I_{DQ}/I_{\Sigma MQ} \tag{3}$$

Finally, it is important to point out that usually in rubber networks, distribution effects of D_{res} (related to different end-to-end separations and polydispersity of network chains) do not play any role[55]. Therefore, the normalized DQ build-up curve of a bulk rubber can be analyzed in the quasi-static limit in terms of a single D_{res} [37],

$$I_{nDQ}(\tau_{DQ}, D_{res}) = \frac{1}{2}(1 - \exp[-\frac{2}{5}D_{res}^{2}\tau_{DQ}^{2}]) \tag{4}$$

However, the complex and heterogeneous PVA network[25,28] structure, in addition to specific effects related to the swollen state of the sample (which is proven to be heterogeneous in polymer networks[56]), leads to large deviations from the inverted Gaussian shape in the studied PVA gels. The actual coupling distribution (related to a microstructurally heterogeneous distribution of constraints) can be evaluated by using fast Tikhonov regularization of the experimental data[39,57-59]. The insert in Figure 1(b) shows the broad distribution of dipolar interactions in PVA networks. It resembles a gamma distribution, and is consistent with observations of very heterogeneous network structures proposed in the literature[25,28]. All the analyzed samples showed a similar distribution shape independently of the number of freezing/thawing cycles.

Since regularization analysis is subject to some limitations[41] (further work about this point is in progress), we have analyzed all build-up curves under the assumption of the gamma distribution of dipolar couplings, that is predicted by the Gaussian distribution of end-to-end separations (but which is screened in bulk elastomers):[37,41]

$$I_{nDQ}(\tau_{DQ}, D_{avg}) = \int_0^\infty \frac{1}{2}(1-\exp[-\frac{2}{5}D_{res}^2\tau_{DQ}^2])\times\frac{2}{\sqrt{\pi}}\sqrt{\frac{27D_{res}}{8D_{avg}^3}}e^{-3D_{res}/(2D_{avg})}\,\mathrm{d}D_{res} \qquad (5)$$

Upon fitting, the integral is evaluated numerically within the curve fitting environment of the Origin software. In using this distribution, we do not want to imply that this distribution is of any significance in the studied structure, the resulting build-up curves merely describes all our experimental build-up data very well, and has the benefit of not introducing an additional fit parameter, yet providing a well-defined average residual coupling D_{avg} (the width of the gamma distribution is directly related to the average).

Note finally that the MQ analysis pertains to the mobile fraction of the cryogels only; this fraction always constitutes the major part of the sample (>80%), the rest being rigid crystallites, the signal of which relaxes rapidly and is not observable under the conditions of the MQ experiment.

Pulsed mixed magic-sandwich echo (MSE). According to previous papers, polymer crystallites act as junctions in PVA networks obtained by freezing/thawing cycles[25-26,28,33]. Solid state NMR is a useful method to characterize polymer crystallinity or phase composition in this type of systems. The main concept is that the crystalline signal usually decays in the first 20 μs of the free-induction decay, therefore the signal detected after the dead time (12 μs in our case) partially conceals this information. Nevertheless in some works, the fraction of protons in a *glassy* state in PVA gels were estimated by monitoring the FID intensity during the first 20 μs,[60-62] which renders these studies qualitative. Different solutions were reported in the literature. Maybe the most important is the use of solid echoes with different echo delays combined with back extrapolation,[63] in order to correct for its inability to fully refocus the dipolar interactions in a multiple-spin system. The certainly best approach is of course the use of a spectrometer with short (1-2 μs) dead time[64].

The use of a magic-sandwich echo (MSE) was recently proposed[43] as a more effective method to refocus the multiple dipolar interactions that lead the fast decay of the initial part of the FID, therefore removing the dead time problem and obtaining a near-quantitative rigid fraction determination in polymer systems. Under the same experimental conditions, differences around 40% in the quantity of rigid phase in PVA compounds were observed comparing FIDs and MSE-refocussed FIDs (data not shown). Figure 2 shows the MSE-FIDs for different total echo duration (realized by increasing the interpulse spacings). The signal decay data is well represented by a Gaussian function (parabolic initial decay) and its extrapolation to t=0 allows us to conclude that the signal loss is negligible (it could be estimated to around 2% on absolute scale, which corresponds to 10% in relative scale).

Note, however, that even for the MSE, the refocusing efficiency breaks when there is molecular motion on its timescale. This may particularly be the case if the observed rigid component is glassy rather than crystalline and close to T_g. Under any condition, irrespective

of temperature, however, the typical decay time upon incrementing the echo was never significantly shorter than the (relatively weak) decay seen in Figure 2, which is ultimately associated with the breakdown of the pulse sequence efficiency due to higher-order imperfections. We thus conclude that all observed "rigid" signal is associated with crystal-like domains – otherwise, a significant signal loss upon going through T_g would have been observed.

So MSE-FID curves were used in order to quantify the fraction of fast-decaying rigid polymer present in PVA gels. The first fast decay (caused by the rigid polymer fraction) in the MSE-FIDs (Figure 2) has a quasi-Gaussian decay, whereas the slower signal decay could be fitted with an exponential function. Therefore the first 140 μs of the normalized MSE-FID curves (unity signal for zero time) were fitted according to equation 6,

$$I_{MSE-FID} = A\exp\left(-\left(\frac{\tau}{T_{2hard}}\right)^{b}\right) + (1-A)\exp\left(-\frac{\tau}{T_{2soft}}\right) \quad (6)$$

In this expression, *A* is the fraction of detectable *rigid* phase in the sample and *b* is an adjustable parameter for a better fitting of the fast decay shape. In all the cases $b\sim2$, i.e., the crystalline fraction is described by a Gaussian function. In addition, to reference the hard polymer phase to the total amount of polymer (instead of the sample fraction), the *A* parameter was corrected according to the actual fraction of polymer in the sample, obtained from saturation recovery experiments (note again that the samples contain residual water), based on the fact that water has a much longer T_1 relaxation time. From such experiments, and assuming no significant NOE transfer between the species on the same timescale, the water content can be obtained from a bi-exponential fit,

$$M_z = D\left(1-\exp\left(\frac{-\tau}{T_{1W}}\right)\right) + (1-D)\left(1-\exp\left(\frac{-\tau}{T_{1P}}\right)\right), \quad (7)$$

where *D* is the water fraction in the sample and T_{1W} and T_{1P} are the longitudinal relaxation time constant of water and polymer respectively (with $T_{1W} >> T_{1P}$). For example, at T=304K,

the relaxation times were T_{1W} =1520 ms and T_{1P}=60 ms for a network with 10% PVA after 7 freezing-thawing cycles. The fast-decaying rigid crystallite signal was not detected in these experiments (the FID was evaluated at a time beyond 50 μs), such that *D* is determined relative to the mobile polymer fraction, i.e., (1–*A*) in eq. (6).

Finally, the *rigid polymer fraction* discussed below is obtained according to

$$\text{Rigid polymer fraction } (\%) = \frac{\text{A}}{(1-\text{D})} 100 \qquad (8)$$

Obviously, for these corrections it is essential to use a recycle delay that is long enough in order to observe the full equilibrium magnetization of the sample (5 times T_{1W} was used as recycle delay in all experiments, i.e. around 7 to 20 s depending on the temperature).

RESULTS AND DISCUSSION

The starting point of our study is the characterization of two isotropic solutions of 10 and 20% (w/v) of PVA in water. The 10% PVA solution does not give any detectable DQ signal, but for the decay (I_{ref}) data, two different processes can be identified, i.e. the decay of the polymer magnetization and the water relaxation. This result demonstrates that under this preparation and measurement conditions, the dilute solution can be considered non-entangled and above the gelation threshold. This is not a trivial result, as DQ experiments are in principle sensitive to transient links (entanglements or hydrogen bonds), and this appears indeed indicated by the 20% PVA solution: under the same preparation conditions, DQ experiments did yield a detectable build-up curve. However, this is in our case due to a non-dissolved or partially gelled PVA subphase. To avoid this problem, 20% PVA solutions were prepared under more vigorous stirring as well as higher temperatures up to 90ºC. In this way, a totally isotropic solution of polymer was obtained according the DQ experiments.

DQ experiments were performed on PVA samples subject to different number of freezing/thawing cycles to determine the evolution of non-coupled network defects as well as the network mesh size according to the advance of the gelation process. In Figure 3 we can see that after the first freezing/thawing cycle, approximately 50% of the polymer chains are coupled and are therefore part of the network, whereas the rest is not linked to it or at least belongs to elastically not active dangling chains or loops. The amount of PVA chains incorporated into the gel network increases with the successive cycles until it reaches a plateau after the 6th cycle, where the network has the minimum defect content. This important result shows that, independently of the number of freezing/thawing cycles applied to a PVA solution, around 25% of the polymer is not coupled, and therefore should not be elastically active. This is a very significant observation that is usually not taken into consideration when mechanical[11,27], dynamic-mechanical[27,31] or rheological[15,24] properties of this material are analyzed. Urushizaki et al.[65] have related the viscoelastic properties of this type of gel with the non-incorporated PVA chains, and they have estimated their amount from the difference in weight between the polymer gel after and before immersion in distilled water. They found that around 10 % of the polymer was not incorporated after the first freezing/thawing cycle. Obviously, our experimental values are much larger because we not only detect the non-crosslinked chains, but also the dangling chains and other non-elastic network defects (e.g. loops).

In addition, the decrease in the number of defects is correlated with an increase in D_{res} that is proportional to the network chain order parameter (Eq. 1), see Figure 4. The formation of crosslinks (independently of their nature) renders the polymer segmental motion non-isotropic, whereby the chain segments become ordered with respect to the end-to-end distance, and residual dipolar couplings arise. According to this basic principle, increase in D_{res} is directly related with the (inverse) length of the chains between the constraints. Similar to the observation for the non-coupled network defects, the network chain length appears to

approach a plateau after cycle number 6, yet the tendency is not as clear as the former result. Even after 16 cycles, the crosslink density still appears to increase.

With this observable, and in contradiction to the current opinion, it is important to note that samples with different polymer concentration appear to exhibit the same behaviour during gelation. The observation is however reasonable in the framework of a heterogeneous scenario, where crosslinking occurs via partial crystallization in the non-frozen parts of the sample, it simply means that in less concentrated samples more water freezes.

However, the freezing time (especially in the first cycle, when the network is formed) seems to have some influence in the gel network structure. As it is shown in Figure 4, the apparent dipolar coupling constant is very low (~48 Hz) after 1 hour of freezing. If the freezing period is increased to 3 hours, the crosslink density of the gel almost doubles (~82 Hz), while longer freezing (e.g. 16 hours) does not lead to any more variation. This may indicate that 1 hour of freezing is not long enough in order to complete the process, and for this reason, further analyses are based on samples with a first freezing cycle of 12 hours and subsequent cycles of 3 hours each.

Coming back to the origin of the PVA networks produced via freezing-thawing cycles from homogeneous polymer solutions in water, it appears to be well demonstrated by now that during the first freezing cycle, freezing of some water[29] increases the concentration in the still unfrozen phase[28]. Crystallization of PVA takes place in this concentrated microphase,[66] but it is kinetically frustrated by gelation of the polymer solution[25,28-29]. This fact could explain the small size of these primary crystallites (around 5 nm),[25-26,28] which then act as physical junctions between the amorphous and mobile polymer chains. Results extracted from the MSE-FID curves of the PVA gels after the first freezing/thawing cycle (Figure 5) indicate that around 8% of the polymer behaves like a rigid solid. This rigid fraction increases with the number of cycles until it reaches a plateau close to cycle number 6, just as our other reported network properties. The maximum amount of rigid phase estimated by our NMR

methodology (around 20% of the total polymer) is substantially higher than the crystallinity of similar samples deduced by DSC[24-25] as well as some other ^{1}H NMR methods[15,25].

The crystallinity of PVA cryo-gels obtained in DSC studies is in all cases estimated to around 5% (not taking into account studies of dry networks,[33] since the structure should be different). However, as was pointed out by Willcox et al.,[25] this magnitude could well be underestimated since the heat of fusion of the crystals in gels may be substantially lower than the assumed PVA bulk value due to their small size and large surface effects (hydrogen bonds to surrounding water, etc.). In addition, another important point is the difficulty to measure small quantities of crystal phase in dilute gels via colorimetric methods in general (for example, a crystallinity of 8% in a gel with a PVA concentration of 20% only represents a sample fraction of 0.016).

For these reasons, the use of solid state NMR seems to be a better methodology to quantify the crystallinity in dilute PVA gels. There are, however, still some discrepancies in the total amount of rigid phase measured by using different NMR methodologies. Ricciardi et al.[15] estimated the crystallinity of PVA gels after 11 freezing-thawing cycles to around 8%, by analyzing the first μs of the ^{1}H FID. Clearly, as was pointed out in the experimental part, this experimental procedure falls victim to the dead time problem. Depending on the spectrometer, the amount of rigid signal lost during this time could be more or less significant (reference 15 does not specify the dead time, therefore it is not possible to estimate the related error). For example, our low field spectrometer has a dead time of around 12μs, therefore the FID analysis would lead to an underestimation of the rigid polymer fraction by about 50%. On the other hand, Willcox et al.,[25] by using different ^{13}C NMR experiments (direct-polarization as well as ^{1}H-^{13}C cross polarization), established that after the first freezing/thawing cycle, PVA gel contains a rigid polymer phase of around 5±2%, increasing up to 12±4% after cycle number 12. These last values are closer to our experimental estimation, but still far away. As was pointed out by the authors,[25] the relative fraction comparing different samples could be

estimated with a high accuracy, but the used methodology (in particularly the use of the intrinsically non-quantitative cross polarization) does not give a reliable absolute crystallinity.

In conclusion, the key to obtain the most accurate crystal fraction in these dilute polymer samples is to use a solid-state NMR method that allows us to fully detect the rigid part by refocusing the multi-spin dipolar interactions with the MSE, thus solving the dead time problem and minimizing the signal loss. Of course, detecting the more sensitive and 100% abundant protons instead of naturally abundant ^{13}C is an additional advantage, which more than compensates for the use of an intrinsically less sensitive low-field spectrometer.

Summing up all results discussed so far, the network structure of PVA cryo-gels is very apparently based upon the formation of rigid polymer areas (most probably polymer crystallites) during the cooling process. After the first cycle, almost half (~8%) of the final amount (20%) of rigid phase is already formed. At this stage, about 50% of the all polymer segments are part of the network structure. Subsequent freezing-thawing cycles increase the rigid polymer fraction, which has two consequences: First, a further reduction of the non-coupled polymer fraction, i.e., more PVA segments become elastically active. Second, the network mesh size is further reduced, but only slightly during further freezing/thawing cycles. Therefore, we believe that subsequent freezing-thawing cycles not only increase the size of the crystals formed during the first freezing process, but also lead to the creation of other more imperfect crystals.

Melting of smaller and more imperfect secondary crystals takes place at lower temperature and over a large range, leading to a continuous decrease in the detected rigid polymer phase with the temperature (Figure 6). At around 75-80 °C (in good agreement with the main endotherm observed in DSC measurements[24-26]), this quantity drops below the detection limit. This should be correlated with the melting of the main (primary) crystals (estimated to about 5% of the polymer fraction), that support the network structure of the gel. These results are consistent with DSC measurements[24-25] as they show an increase in the

melting endotherm, corresponding to the initial crystals as well as the appearance of a second endotherm at lower temperatures when the number of freezing/thawing cycles was increased for a given PVA solution.

The effect of the number of freezing-thawing cycles on the crystallinity is easily understandable by comparing the evolution of the rigid polymer fraction of a PVA gel obtained after 7 cycles with a PVA gel after only 1 freezing/thawing cycle (Figure 6). The onset of melting after only 1 freezing cycle is estimated to around 50°C, leaving the rigid polymer fraction constant at lower temperatures. Therefore, subsequent cycles seem to create more, yet imperfect secondary crystallite structures. Above 50°C all samples exhibit a similar behaviour, related with the partial melting of primary crystals or with the melting of less perfect secondary structures. Importantly, the temperature above which it is not possible to detect any more signal of rigid polymer remains invariant, yet the final fraction seems to increase slightly with the number of cycles. Therefore, according to this result, freezing/thawing cycles have a direct influence on the amount of crystals formed during the first freezing process, but also the creation of other more imperfect secondary crystallites.

Here it is important to note that polymer concentration of the original solution does not have any effect on both studied processes, i.e., on the formation of the rigid polymer phase with the freezing-thawing cycles, as well as on the progressive melting of this phase upon increasing temperature. Again, this is consistent with the notion that simply less water freezes at higher concentration. In this context, it appears worthwhile studying the influence of the actual freezing temperature, which should affect the polymer concentration under the conditions when the crystallites are formed.

To ensure that the results shown in Figure 6 are not artefacts produced by different magnetization relaxation at different temperatures, as possibly arising from regions that undergo a glass-to-liquid rather than a melting transition, the evolution of the signal at any given temperature was studied as a function of echo delay, see Figure 7. At all the measured

temperatures, similar behaviour was found, with a loss of intensity estimated to between 0.7 and 1.8% for the two extreme cases, which corresponds to a constant 10% loss on a relative scale, as is usually found. Importantly, the drop in overall signal corresponds, within the error margins, to the expected drop due to the Curie factor (temperature dependent spin polarization). In addition, a direct check is the control of the total intensity, comparing the PVA gels with the corresponding PVA solutions (insert in Figure 7). It is seen that no significant signal is lost/undetectable (we observe almost all protons in the sample), and from this, it is clear that the loss of intensity caused by the MSE in PVA gels is at a minimum, with no other (hidden) phenomena that could be related to an intermediately mobile (almost glassy) rigid fraction. Given this experimental evidence, the decay of the rigid ^{1}H fraction with temperature can only be related to a melting of PVA crystallites.

Obviously, temperature-dependent variation of rigid polymer phase has a direct effect on the network structure, as is shown in Figure 8. Melting of secondary crystals leads to an almost exponential increase in the number of network defects (obviously in a reversible pathway, comparing the phenomenon with the effect of successive freezing/thawing cycles). However, the network mesh size (as measured by the residual dipolar coupling) remains almost constant. This means that secondary crystallization is very important in the network organization, reducing the number of network defects and therefore increasing the amount of polymer segments that are elastically active. However, the molecular weight between the constraints appears to be mostly dictated by the primary crystallites formed during the first freezing cycles. For this reason, the network is completely destroyed at temperatures around 80ºC when the primary crystal phase is molten, leaving no observable DQ signal (i.e. an isotropic PVA solution is formed). On the side, we note that the differences in the D_{avg} values given in Figures 4 and 8(b), which indicate a 50% decreased mesh size for the samples studied in Figure 8, is related to the increase in the freezing time (12h in the first step and 3h in the successive cycles instead of 1h) used in each cycle, as pointed out above.

These NMR results on the mesh size agree perfectly with the trends observed in studies of mechanical properties reported in the literature. Clearly, the elastic behaviour of PVA gels depends on the number of freezing/thawing cycles[15,27,31,65]. The crystallinity increases, while the mesh size is only slightly reduced. Therefore, the main factor that determines the improvement of the mechanical properties upon further cycles should be associated with the number of elastically active chains. The polymer concentration in the original aqueous solution has an important effect on the elastic properties[15,31], i.e., the elastic modulus increases. However, in the view of our data, this does not appear to have important consequences for the actual network structure, i.e., there are no large variations in the network mesh size, therefore the reported variations are simply related to differences in polymer concentration. In addiction, different works[31,65] demonstrate a slight decrease in the elastic modulus with the temperature, until a major drop occurs at 50°C.[65] This is obviously related to the partial melting of secondary and more imperfect crystallites that leads to an increasing amount of network defects (elastically inactive chains). At temperatures close to 80°C, the complete loss of crystallinity essentially liberates all chains and the system drops below the gelpoint. In view of the important role of the substantial polymer amount that is not elastically active (free and dangling chains, loops), it may be worthwhile to re-consider detailed frequency-dependent mechanical measurements, where these components should contribute to an increased loss modulus over the frequency range covering their relaxation.

The capacity of our investigated systems to be transformed from an isotropic aqueous solution to a physical cryo-gel by application of freezing/thawing cycles, including thermal reversibility back to an isotropic PVA solution, is in clear contradiction with the assertion that covalent bonds could form between the polymer chains during gelation.[30] If covalent crosslinks were an important contribution to the final gel properties, residual couplings should persist even above the melting temperature of the crystallites, which is not the case. However, the presence of (rapidly tumbling) microgels above the main melting point cannot be ruled

out, and is in fact indicated by the relatively high viscosity (as checked by a simple tilt test). However, we point out that even the pristine 20% PVA solution exhibited some detectable DQ signal, indicating extended gel-like structures, unless it was heated above 90°C. Therefore, an undetectably small fraction of crystallites (or extended hydrogen-bonded aggregates) may always be present even above 80°C, and hold the system close to the gel point, depending on the sample and its thermal history. From our perspective, permanent bonds can be ruled out as a major factor determining the cryo-gel structure.

Finally, we address ageing phenomena, that are part of the data shown in Figure 6 and were not commented on until now: after heating a sample containing 10% of PVA up to 50°C and recording the loss of crystallinity, the sample was stored for 12 hours and another measurement was performed at room temperature. The amount of rigid polymer fraction after 12 hours of storage was again increased considerably, as can be seen in Figure 6. Yet, this new crystalline fraction melts at rather low temperatures, which again indicates the growth of secondary crystallites. Similar prominent ageing effects have been reported in the literature.[4,25-27,31]

For more clear evidence, a sealed sample containing 20% of PVA was submitted to 7 freezing/thawing cycles (with 12 hours of freezing in the first cycle), and characterized after different storage times at room temperature. According to Figure 9, ageing clearly increases the secondary population of imperfect crystals. It also increases the amount of elastically active polymer segments, but has no significant effect on the network mesh size. Therefore, ageing effects on PVA gel properties[4,25-27,31] are again mainly related to an increasing fraction of polymer incorporated into the network structure, and not to a decrease in mesh size.

CONCLUSIONS

Poly(vinyl alcohol) (PVA) hydrogels obtained by freezing-thawing cycles exhibit a complex heterogeneous network structure. This physical gel is supported by rigid polymer areas (PVA crystallites), that act as junctions between the remaining mobile and entropically elastic polymer chains, and thus determine the network mesh size. In our study, the crystallites are quantitatively detected as a rigid-like fraction of quickly relaxing (and fully refocussed, to overcome the dead-time problem) magnetization, and the mesh size is deduced from multiple-quantum experiments that measure residual dipolar couplings, the latter arising from constraints to the motion of the mobile chains (=crosslinks) that render the segmental motion locally anisotropic.

The most important crystal fraction forms in the first freezing cycle, and subsequent freezing/thawing cycles only produce a slight increase in the initial crystal size as well as induce the formation of more imperfect, secondary crystallites. This secondary crystal fraction (which constitutes around 2/3 of the total crystal phase in samples submitted to a large number of cycles and/or extended aging), plays an important role by increasing the number of elastically active polymer chains, but it does not appreciably affect the mesh size. This effect also diminishes when longer freezing cycles are applied.

PVA cryo-hydrogels are shown to be totally thermo-reversible, i.e. PVA physical networks can be transformed into an isotropic aqueous solution by increasing the temperature. During this process, the more imperfect crystals are molten first, and the number of network defects increases exponentially. In contrast, the network mesh size does not undergo significant variations until the primary crystal phase is molten at temperatures around 80 ºC. Our experiments did not reveal any evidence on the possible formation of covalent crosslinks between PVA chains during gelation; no residual couplings were detected after the melting of this primary crystal fraction.

Independently of the number of cycles, ageing and/or the polymer concentration in the original PVA solution, a considerable fraction of polymer (25% at least) is not elastically

active, which is a result as yet not taken into account in the large body of literature addressing the formation and the properties of PVA cryo-hydrogels. This finding is central to the interpretation and understanding of the elastic properties of this useful material, and must be taken into account in a re-interpretion of the origin of the changes of the elastic moduli of PVA cryogels.

Finally, it is important to note that the in-depth study of both processes, i.e. the PVA gelation by application of freezing/thawing cycles, as well as the destruction of the network structure by heating, were entirely based upon the use of an un-expensive low-field solid state NMR spectrometer. We show that the combination of different advanced NMR strategies, i.e. MQ spectroscopy and component analysis of MSE-refocused free-induction decays, is vital to obtain quantitative information on network structure and phase composition (crystallinity), respectively, in order to arrive at conclusions that can be matched up with information extracted from other diverse techniques.

ACKNOWLEDGMENT

JLV wants to thank the Alexander von Humboldt Foundation as well as the Ministerio de Educacion y Ciencia (Spain) for his fellowships. KS acknowledges financial support by the Deutsche Forschungsgemeinschaft (DFG, SFB 418 and SA982/1-2).

FIGURE 1

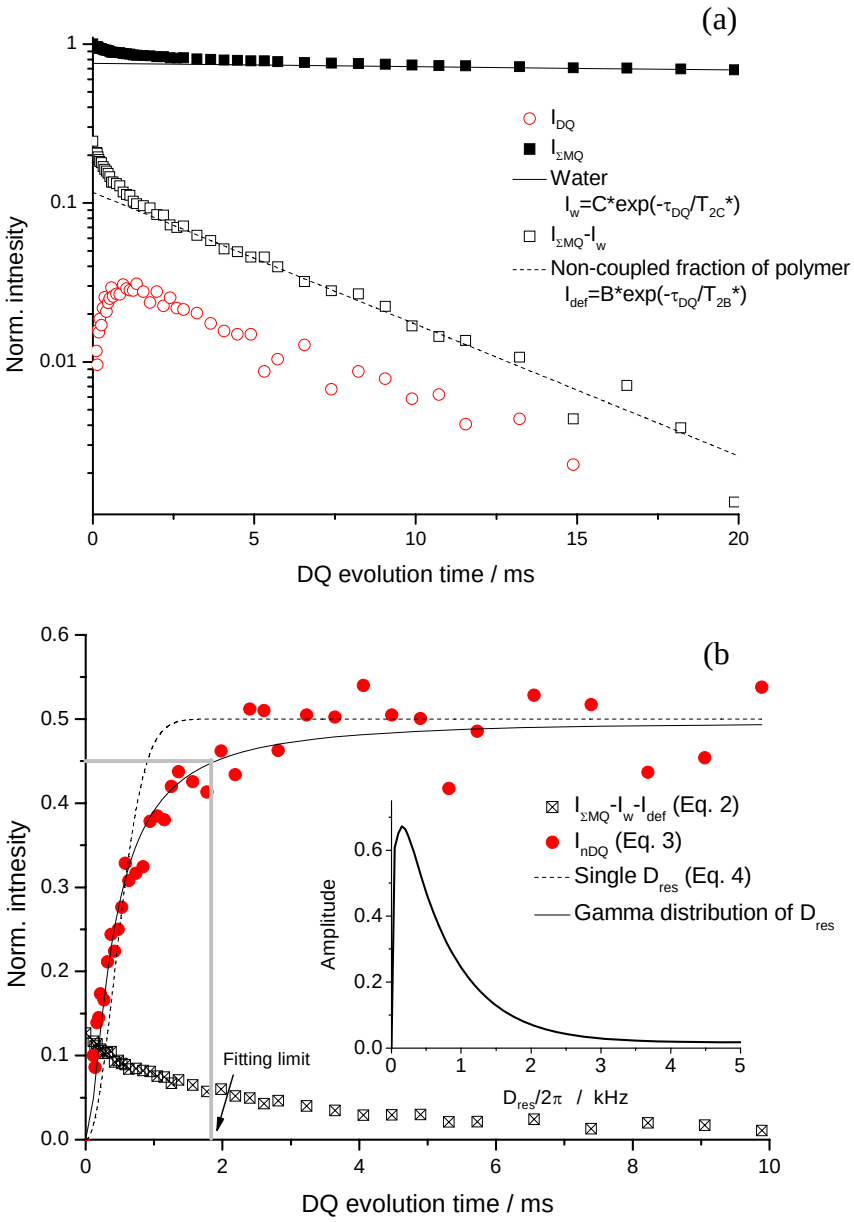

Figure 1. MQ NMR build-up and decay data for 10% PVA sample after 1 freezing/thawing cycle. (a) As-acquired I_{DQ} and $I_{\Sigma MQ}$, and (b) $I_{\Sigma MQ}$ (after extraction of non-coupled contributions) and normalized DQ build-up curve (I_{DQ}). The solid line in (a) represents the exponential fit for water subtraction and the dashed line is the exponential fit representing the subtracted non-coupled polymeric defects. In (b), solid and dashed lines represent the fits assuming a gamma distribution of D_{res} and a single residual dipolar constant, respectively. The insert is the result of a numerical analysis of I_{nDQ} via Tikhonov regularization.

FIGURE 2

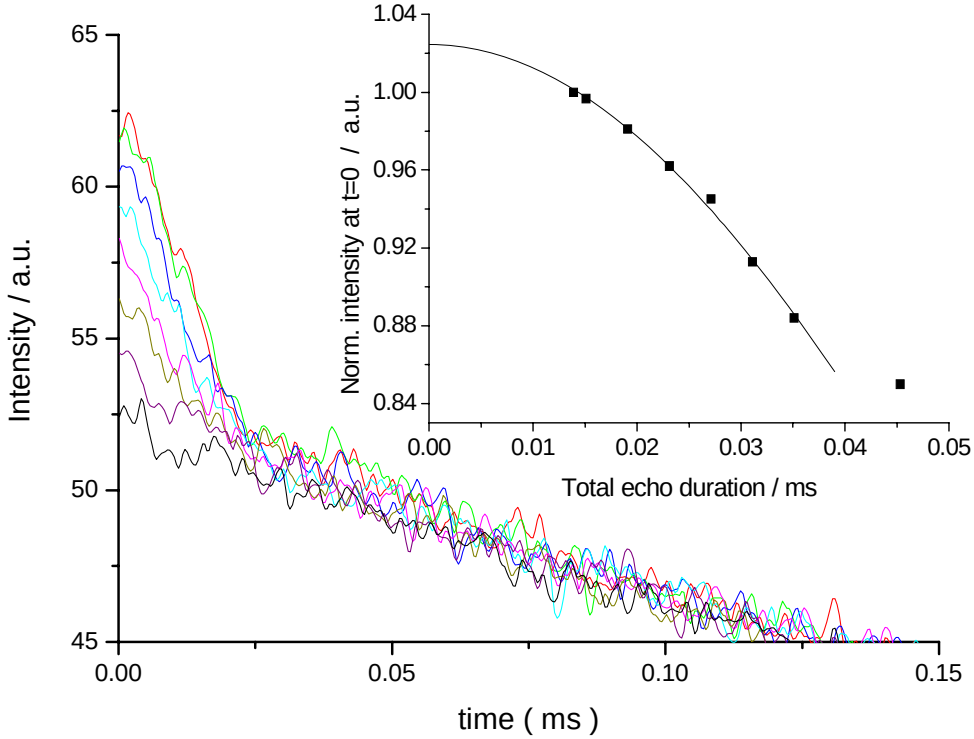

Figure 2. MSE-refocussed FIDs of 10% PVA gel after 6 cycles, measured at different echo time. Inserted graph shows a parabolic (Gaussian) extrapolation of the intensity to time t=0, indicating only minor losses of rigid signal at the shortest echo time (10% on a scale relative to the total crystallinity).

FIGURE 3.

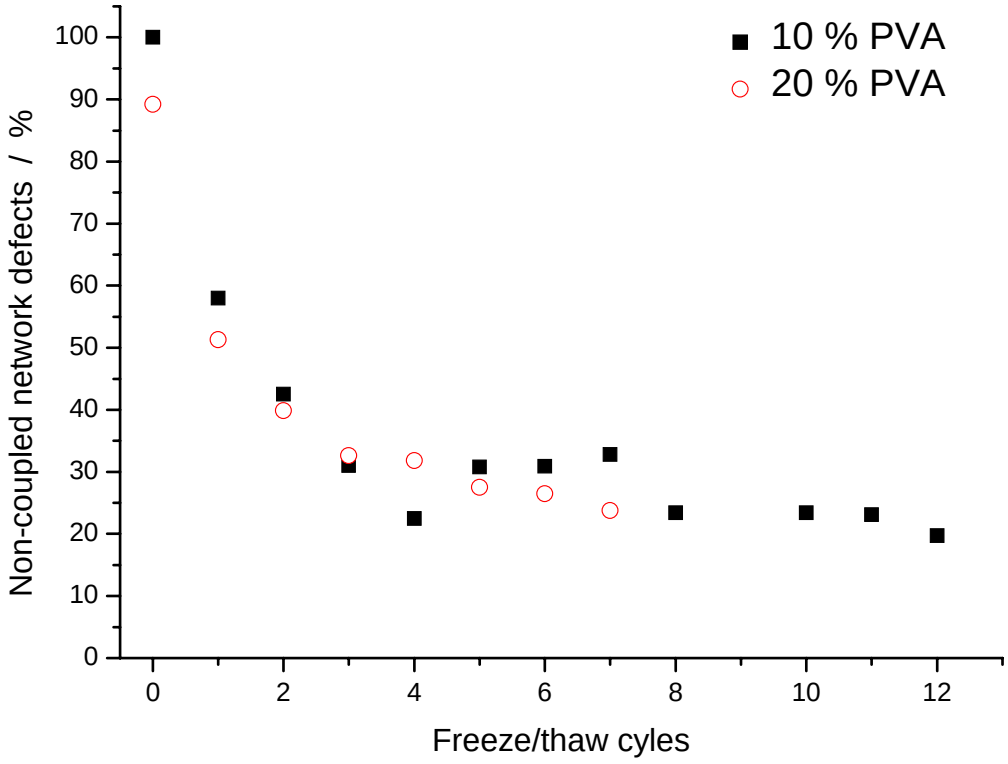

Figure 3. Variation of non-coupled network defects (i.e., non-crosslinked polymer chains, dangling chains and loops) as a function of the number of freezing/thawing cycles for the studied PVA solutions.

FIGURE 4

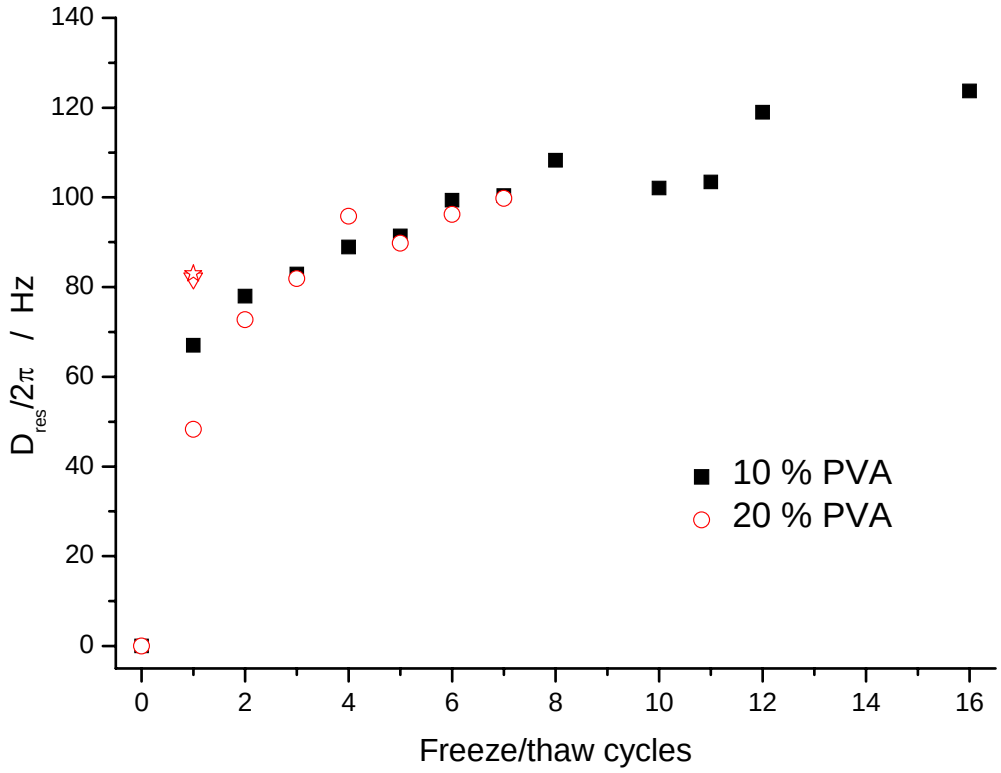

Figure 4. Variation of the average residual dipolar couplings (directly related to 1/N, and therefore the crosslink density or the inverse mesh size) extracted from DQ experiments as a function of the number of freezing/thawing cycles for the studied PVA solutions. The triangle represents a sample containing 20% PVA after 3 hours of freezing, and the star is from the same sample after 16 hours of freezing.

FIGURE 5

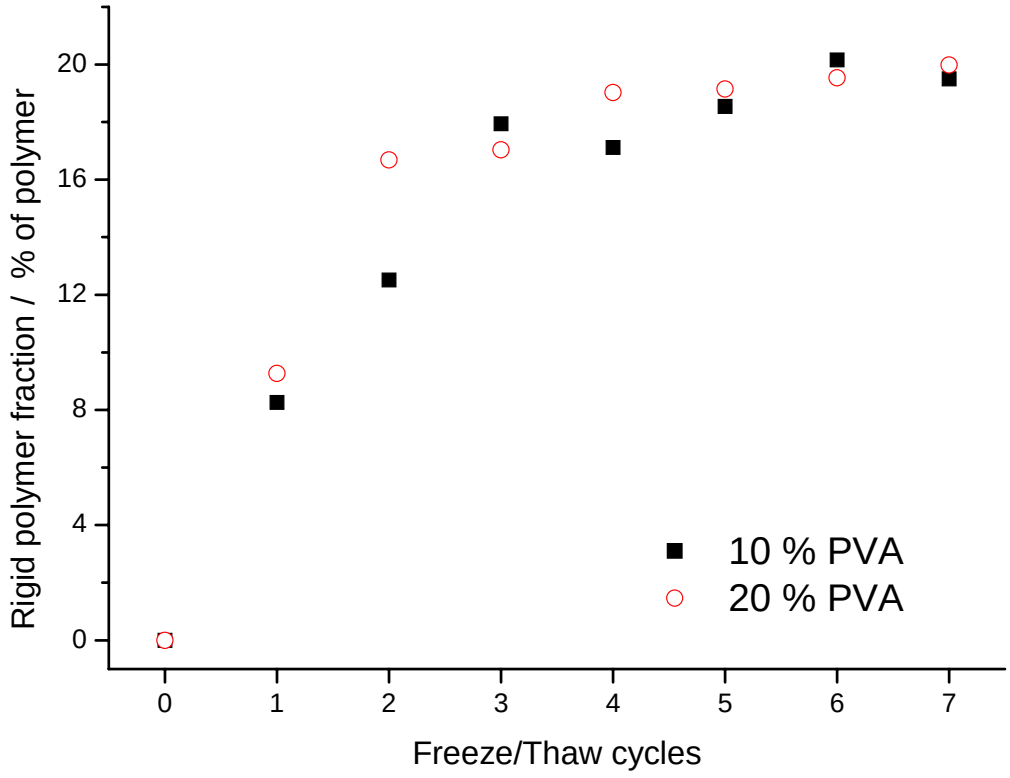

Figure 5. Variation of the rigid (crystalline) polymer fraction extracted from MSE-FID curves as a function of the number of freezing/thawing cycles for the studied PVA solutions.

FIGURE 6

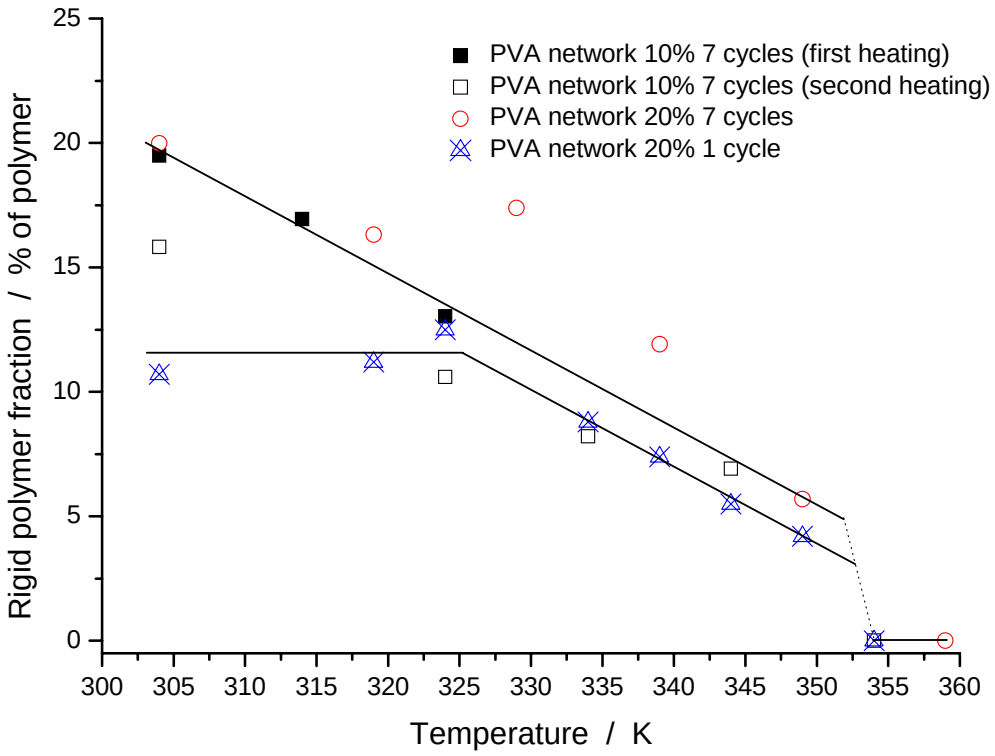

Figure 6. Variation of the rigid polymer fraction (extracted from MSE-FID experiments) as a function of temperature for PVA gels formed after 7 freezing/thawing cycles. A network with 10% of PVA was first heated until 324 K (full squares) and then kept at room temperature for 12 hours before the second heating procedure was performed (empty squares). A solution with 20% PVA was submitted to two different treatments, i.e. 1 freezing/thawing cycle and 7 freezing-thawing cycles, respectively. Lines are only guides to the eye. All samples were frozen for 12 hours in the first cycle and 3 hours in the subsequent cycles.

Figure 7.

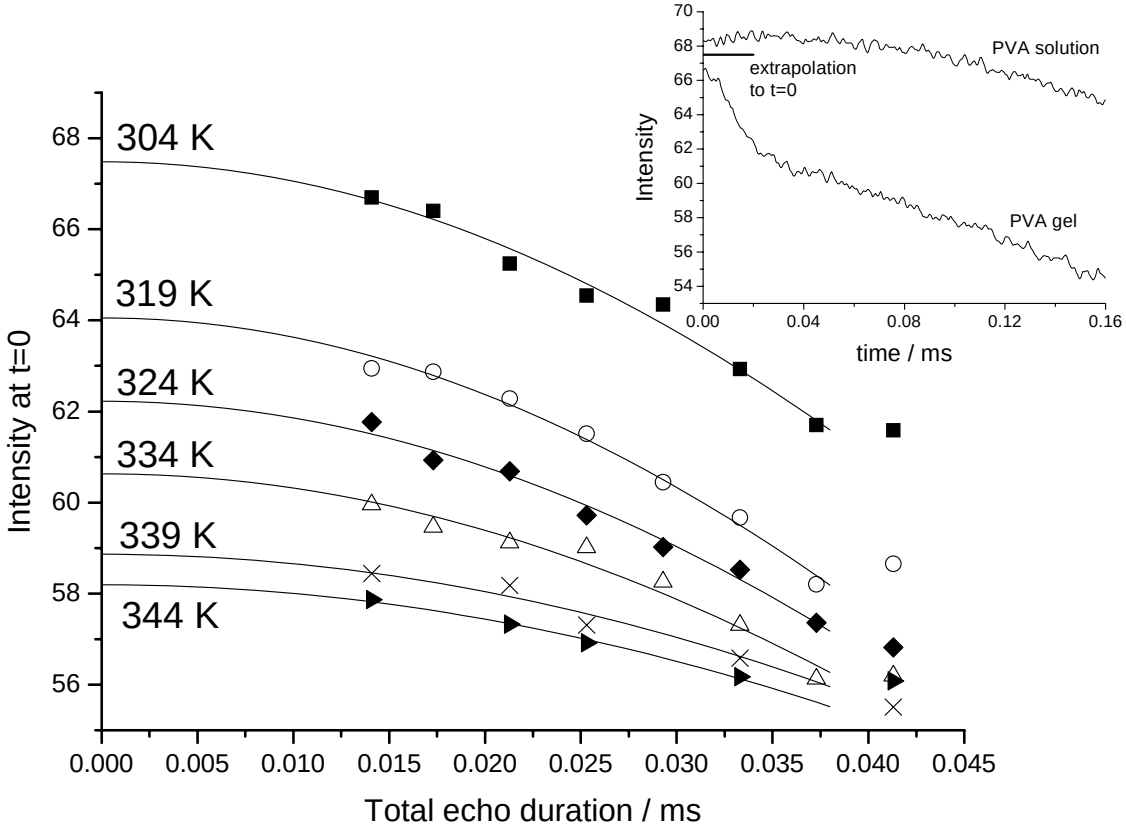

Figure 7. Variation of the initial signal intensity of MSE-FIDs with increasing echo delay at different temperatures for a PVA gel containing 20% polymer after 1 freezing/thawing cycle (12 hours of freezing and 1 hour thawing). Lines are the result of parabolic fits. The insert presents the MSE-FID of the PVA gel measured at 304K with the minimum echo delay (0.0022 ms), as well as the estimated intensity at zero echo time, in comparison to the MSE-FID of the isotropic solution of the same sample measured under the same conditions (after complete melting at 90°C).

FIGURE 8

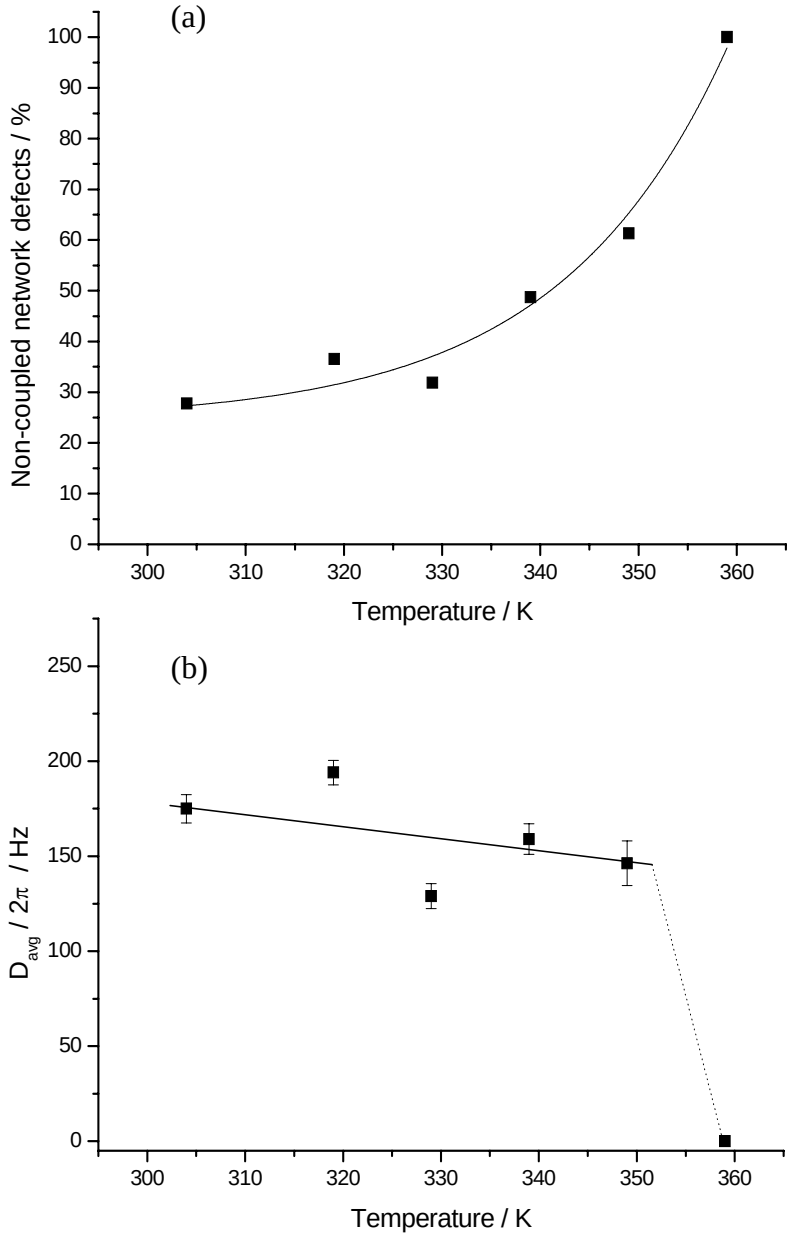

Figure 8. Variation of (a) the network defect fraction and (b) the inverse mesh size (given by D_{avg} measured by MQ NMR) with temperature for the 20 % PVA gel prepared after 7 freezing/thawing cycles (12 hours first freezing cycle, 3 hours subsequent cycles). Error bars represent the fitting uncertainty whereas lines are only guides to the eye.

Figure 9.

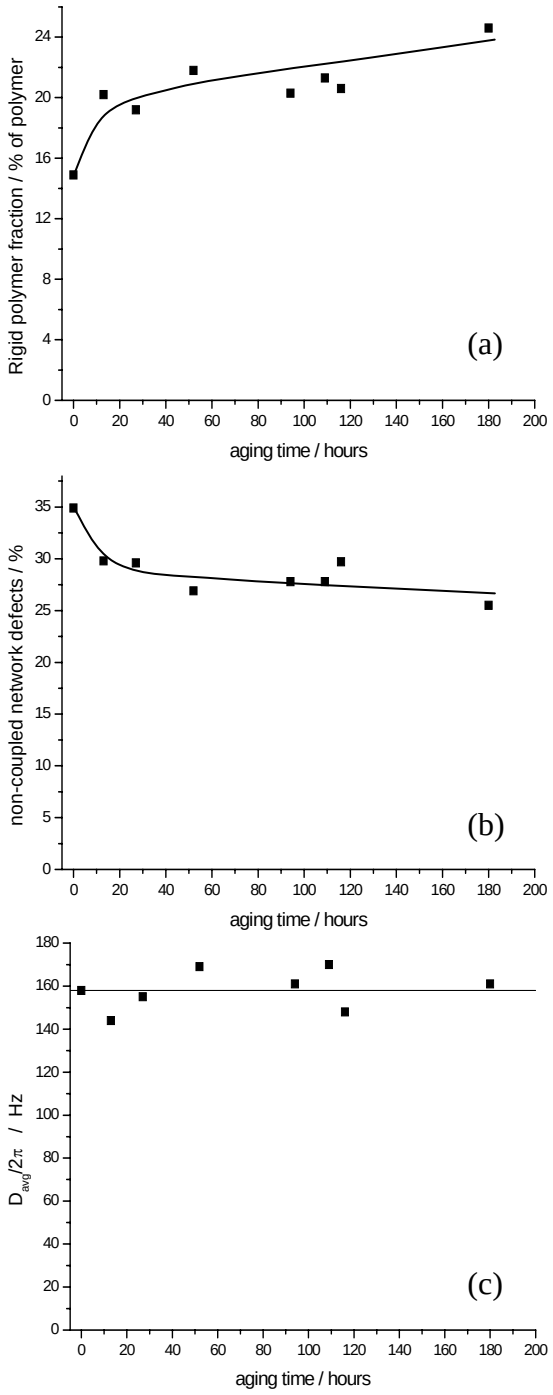

Figure 9. Effect of ageing on (a) the rigid polymer fraction, (b) the non-coupled defects fraction, and (c) the average residual dipolar coupling of a gel with 10% of PVA obtained after 7 freezing/thawing cycles (12 hours of freezing for the first cycle and 3 hours for the following cycles). All properties were measured at 30°C. Lines are only guides to the eye.

BIBLIOGRAPHY

1. K. H. Schmedlen, K.S. Masters, J. L. West. *Biomaterials*. **2002**, 23, 4325-4332.
2. M. C. Doria-Serrano, F. A. Ruiz-Trevino, C. Rios-Arciga, M. Hernandez-Esparza, P. Santiago. *Biomacromolecules*. **2001**, 2, 568-574.
3. C. M. Hassan, J. E. Stewart, N. A. Peppas. *Eur J Pharm Biopharm.* **2000**, 49, 161-165.
4. C. M. Hassan, N. A. Peppas. *Adv. Polym. Sci*. **2000**, 153, 37-65.
5. J. M. Guenet. *Thermoreversible Gelation of Polymers and Biopolymers.* London: Academic Press; 1992.
6. K. T. Nijenhuis. *Adv. Polym. Sci.* **1997**, 130, 1-12.
7. N. A. Peppas. *Makromol. Chem.* **1975**, 176, 3433-3440.
8. E. Pines, W. Prins. *Macromolecules*. **1973**, 6, 888-895.
9. G. T. Feke, W. Prins. *Macromolecules*. **1974**, 7, 527-530.
10. M. Komatsu, T. Inoue, K. Miyasaka. *J. Polym. Sci. B: Polym. Phys.* **1986**, 24, 303-311.
11. S. R. Stauffer, N. A. Peppas. *Polymer.* **1992**, 33, 3932-3936.
12. A. S. Hickey, N. A. Peppas. *J. Membrane Sci.* **1995**, 107, 229-237.
13. N. A. Peppas, J. E. Scott. *J. Control. Release*. **1992**, 18, 95-100.
14. R. Ricciardi, F. Auriemma, C. de Rosa. *Macromol. Symp.* **2005**, 222, 49-63.
15. R. Ricciardi, C. Gaillet, G. Ducouret, F. Lafuma, F. Lauprete. *Polymer*. **2003**, 44, 3375-3380.
16. V. I. Lozinsky, F. M. Plieva. *Enzyme Microb. Tech.* **1998**, 23, 227-242.
17. V. I. Lozinsky, I. Y. Galaev, F. M. Plieva, I. N. Savinal, H. Jungvid, B. Mattiasson. *Trends Biotechnol.* **2003**, 21, 445-451.
18. V. I. Lozinsky, E. V. Solodova, A. L. Zubov, I. A. Simenel. *J. Appl. Polym. Sci.* **1995**, 58, 171-177.

19. V. I. Lozinsky, L. G. Damshkaln, B. L. Shaskol'skii, T. A. Bubushkina, I. N. Kurochkin, I. I. Kurochkin. *Colloid J.* **2007**, 69, 747-764.
20. V. I. Lozinsky, L. G. Damshkaln, I. N. Kurochkin, I. I. Kurochkin. *Colloid J*. **2008**, 70, 189-198.
21. W. Wu, M. Shibayama, S. Roy, H. Kurokawa, L. D. Coyne, S. Noruma, R. Stein. *Macromolecules*. **1990**, 23, 2245-2251.
22. A. L. Kjoniksen, B. Nyström. *Macromolecules*. **1996**, 29, 7116-7123.
23. F. Yokoyama, I. Masada, K. Shimamura, T. Ikawa, K. Monobe. *Coll. Polym. Sci.* **1986**, 264, 595-601.
24. M. Watase, K. Nishinari. *J. Polym. Sci. Polym. Phys. Ed.* **1985**, 23, 1803-1811.
25. P. J. Willcox, D. W. Howie JR., K.Schidt-Rohr, D. A. Hoagland, S. P. Gido, S. Pudjijanto, L. W. Kleiner, S. Venkatraman. *J Polym Sci. B: Polym. Phys.* **1999**, 37, 3438-3454.
26. R. Ricciardi, F. Auriemma, C. de Rosa, F. Laupretre. *Macromolecules.* **2004**, 37, 1921-1927.
27. R. Ricciardi, G. D'Errico, F. Auriemma, G. Ducouret, A. M. Tedeschi, C. de Rosa, F. Laupretre, F. Lafuma. *Macromolecules*. **2005**, 38, 6629-6639.
28. F. Auriemma, C. de Rosa, R. Triolo. *Macromolecules*. **2006**, 39, 9429-9434.
29. F. Auriemma, C. de Rosa, R. Ricciardi, F. Lo Celso, R. TRiolo, V. Pipich. *J. Phys. Chem. B*. **2008**, 112, 816-823.
30. R. Hernandez, D. Lopez, C. Mijangos, J. M. Guenet. *Polymer*. **2002**, 43, 5661-5663.
31. R. Hernandez, A. Sarafian, D. Lopez, C. Mijangos. *Polymer*. **2004**, 46, 5543-5549.
32. R. Hernandez, M. Rusa, C. C. Rusa, D. Lopez, C. Mijangos, A. E. Tonelli. *Macromolecules*. **2004**, 37, 9620-9625.
33. C. M. Hassan, N. A. Peppas. *Macromolecules*. **2000**, 33, 2472-2479.

34. V. M. Litvinov, P. P. De. *Spectroscopy of Rubbers and Rubbery Materials*. Rapra Technology Ltd. Shawbury, United Kingdom, **2002**.

35. G. Simon, H. Schneider. *Makromol Chem Macromol Symp*. **1991**, 52, 233-246.

36. D. E. Demco, S. Hafner, C. Fülber, R. Graf, H. W. Spiess. *J. Chem. Phys*. **1996**, 105, 11285-11296.

37. K. Saalwächter. *Prog. Nucl. Magn. Reson. Spectrosc.,* **2007**, 51, 1-35.

38. R. Graf, D. E. Demco, S. Hafner, H. W. Spiess. *Solid State Nucl. Magn. Reson*. **1998**, 12, 139-152.

39. M. Schneider, L. Gasper, D. E. Demco, B. Blümich. *J. Chem. Phys*. **1999**, 111, 402-415.

40. K. Saalwächter, M. Gottlieb, R. Liu, W. Oppermann. *Macromolecules*. **2007**, 40, 1555-1561.

41. K. Saalwächter, P. Ziegler, O. Spyckerelle, B. Haidar, A. Vidal, J. U. Sommer. *J. Chem. Phys.* **2003**, 119, 3468-3482.

42. K. Saalwächter, A. Heuer. *Macromolecules*. **2006**, 39, 3291-3303.

43. A. Maus, C. Hertlein, K. Saalwächter. *Macromol. Chem. Phys.* **2006**, 207, 1150-1158.

44. C. Hedesiu C, D. E. Demco, R. Kleppinger, A. A. Buda, B. Blumich B, K. Remerie, V. M. Litvinov. *Polymer*. **2007**, 48, 763-777.

45. B. Blumich, P. Blumler, G. Eidmann, A. Guthausen, R. Haken, U. Schmitz, K. Saito, G. Zimmer. *Magn. Reson. Imaging.* **1998**, 16, 479-484.

46. J. P. Cohen-Addad, R. Vogin. *Phys. Rev. Lett*. **1974**, 33, 940-943.

47. J. P. Cohen-Addad. *Macromolecules*. **1989**, 22, 147-151.

48. J. P. Cohen-Addad. *Prog. NMR Spectrosc*. **1993**, 25, 1-316.

49. V. M. Litvinov. *Macromolecules*. **2006**, 39, 8727-8741.

50. J. Collignon, H. Sillescu, H. W. Spiess. *Colloid Polym. Sci*. **1981**, 259, 220-226.

51. P. T. Callaghan, E. T. Samulski. *Macromolecules*. **1997**, 30, 113-122.

52. E. Fischer, F. Grinberg, R. Kimmich, S. Hafner. *J. Chem. Phys*. **1998**, 109, 846-854

53. R. Graf, A. Heuer, H. W. Spiess. *Phys. Rev. Lett*. **1998**, 80, 5738-5741.

54. K. Saalwächter, B. Herrero, M. A. López-Manchado. *Macromolecules*. **2005**, 38, 9650-9660.

55. K. Saalwächter, J.-U. Sommer, *Macromol. Rapid Commun*. **2007**, 28, 1455-1465.

56. K. Saalwächter, F. Kleinschmidt, J. U. Sommer. *Macromolecules*. **2004**, 37, 8556-8568.

57. J. Weese. *Comput. Phys. Commun.* **1992**, 69, 99-111.

58. J. Weese. *Comput. Phys. Commun.* **1993**, 77, 429-440

59. T. Roths, M. Marth, J. Weese, J. Honerkamp. *Comput. Phys. Commun.* **2001**, 139, 279-296.

60. G. Feio, J. P. Cohen-Addad. *J. Polym. Sci. B. Polym. Phys.* **1988**, 26, 389-412.

61. G. Feio, G. Buntinx, J. P. Cohen-Addad. *J. Polym. Sci. B. Polym. Phys.* **1989**, 27, 1-24.

62. R. H. Ebengou, J. P. Cohen-Addad. *Polymer*. **1994**, 35, 2962-2969.

63. V. M. Litvinov, J. P. Penning. *Macromol. Chem. Phys.* **2004**, 205, 1721-1734.

64. E. W. Hansen, P. E. Kristiansen, B. Pedersen. *J. Phys. Chem. B.* **1998**, 102, 5444-5450.

65. F. Urushizaki, H. Yamaguchi, K. Nakamura, S. Numajiri, K. Sugibayashi, Y. Morimoto. *Int. J. Pharm.* **1990**, 58, 135-142.

66. R. Ricciardi, G. Mangiapia, F. Lo Celso, L. Padano, R. Triolo, F. Auriemma, C. de Rosa, F. Laupretre. *Chem. Mater.* **2005**, 17, 1183-1189.